Available online at www.sciencedirect.com

SciVerse ScienceDirect

Procedia Engineering 21 (2011) 311 – 318

Procedia Engineering

www.elsevier.com/locate/procedia

2011 International Conference on Green Buildings and Sustainable Cities

Investigation of a Hybrid Solar Heat Pump System

Hongbing Chen[a,b*], Saffa B Riffat[b]

[a]*Beijing University of Civil Engineering and Architecture, 1 Zhanlanguan Road, Beijing 100044, China*
[b]*University of Nottingham, University Park, Nottingham NG7 2RD, UK*

Abstract

Many studies found that the decrease in photovoltaic (PV) cell temperature by 10 ℃ can improve the efficiency by 0.5-0.7% based on the reference efficiency of 15%. In this paper, the refrigerant R134a was used to cool down the PVs and thus improve the electrical efficiency. A hybrid flat plate PV panel, made of a glass cover – PV module – alluminium sheet – copper tube – insulation – metal sheet sandwich, was coupled with a heat pump system acting as the evaporator. Numerical models were established for the performance study. The results indicated that electrical efficiency dropped by 0.005 and thermal efficiency increased by 0.03 with every 100 W/m^2 increase of radiation. The maximum COP could reach 6.6.

Keywords: Photovoltaic/thermal collector; Heat pump system; COP;

1. Introduction

Photovoltaic (PV) technology has been widely used for generating electricity. However, the PV modules are inefficient in terms of solar-to-electricity conversion efficiency, less than 20% for commercial PV modules [1]. Many studies found that the decrease of PV cell temperature would increase the solar-to-electricity conversion efficiency. In order to improve the electrical efficiency, many researchers employed air [2-3] and water [4-5] to cool down the PV modules, and the heat extracted from the PVs was used for space heating or domestic hot water supply. It was found that water was better than air in terms of PV cooling and energy performance but the improvement made by PV cooling was small.

In this study, the refrigerant R134a was used as the cooling liquid for the cooling of flat plate PV panel. The PV panel, acting as the evaporator, was coupled with a heat pump system. The small portion

* Corresponding author. Tel.: +44-115-8467676; fax: +44-115-9513159
E-mail addresses: Hongbing.Chen@nottingham.ac.uk

doi:10.1016/j.proeng.2011.11.2020

Nomenclature

A	area (m^2)
Cp	specific heat at constant pressure (J kg^{-1} K^{-1})
d	diameter of copper pipe (m)
E	photovoltaic power per unit surface area (W m^{-2})
f	packing factor of the PV module
G	solar irradiance (W m^{-2})
h	specific enthalpy (kJ kg^{-1})
m	mass flow rate (kg s^{-1})
P	pressure (Pa)
q	heat flux (W m^{-2})
T	temperature (K)
u	flow velocity (m s^{-1})
V	volume (m^3)
v	specific volume (m^3 kg^{-1})
x	refrigerant dryness fraction

Greek letters

α	convective heat transfer coefficient (W m^{-2} k^{-1})
κ	compression index
δ	thickness (m)
η	efficiency
λ	thermal conductivity (W m^{-1} k^{-1})
μ	dynamic viscosity (pa s)
ρ	density (kg m^{-3})
σ	Stefan-Boltzmann constant (W m^{-2} k^{-4})
τ	transmittance
$\beta\tau$	effective absorptance

Subscripts

a	air
al	aluminium sheet
bp	PV base plate
c	solar cells
cd	condenser
co	copper tube
com	compressor
d	heat conduction
dis	discharge
ev	evaporator
g	glass vacuum tube
hx	heat exchanger
i	inner
o	outer
p	PV module
r	refrigerant; heat radiation
w	water

of the absorbed solar energy was converted to electricity. The rest energy was converted to waste heat, extracted by the refrigerant at the back surface of the PV panel. After the Rankine refrigeration cycle operation, the heat was released later at the condenser. With the low evaporating temperature, it was expected to achieve better cooling effect and better electrical performance of the PV modules. Numerical study on energy performance of a hybrid flat plate PV heat pump system was carried out.

2. System descriptions

The hybrid PV heat pump system comprises four main parts: compressor, expansion valve and water-cooled condenser as well as PV panel (evaporator). The PV evaporator is the key component, which is different from that of conventional heat pump systems. Fig.1 shows the layout of the flat plate PV panel. The flat plate PV panel is made of a flat plate type glass cover – PV module – aluminum sheet – copper tube – insulation – metal sheet sandwich. A cross-sectional view of part of the flat plate PV panel is shown in Fig.2. At the panel, a flat plate PV module is used as thermal absorber, with refrigerant copper tube running underneath. The tube is firmly fixed between PV module and aluminum sheet under precise pressure control to provide a good contact between the aluminum sheet and the copper tube. This enables a good heat transfer from the aluminum sheet to the refrigerant. The copper tube pitch was 50 mm. Thermal insulation is provided at the back of the PV panel to minimize heat loss. The PV modules are adhered on top of the base plate with glass cover. The total aperture area and PV cell area were 0.65 m2 and 0.49 m2, respectively.

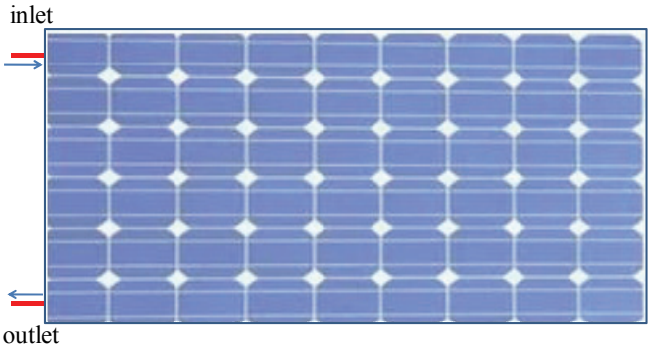

Fig. 1. Layout of the flat plate PV panel.

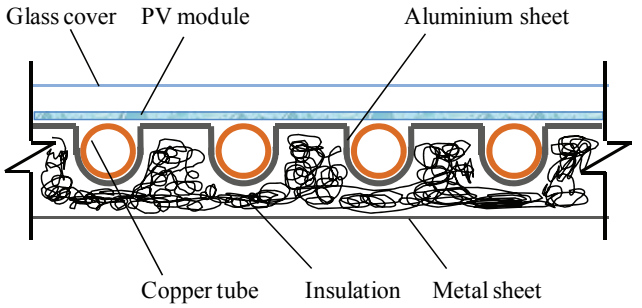

Fig. 2. Cross-sectional view of part of the flat plate PV panel

3. Numerical models

Zondag et al. [6] built four numerical models for the simulation of PV/T collector: a 3D dynamical model and three steady state models that are 3D, 2D and 1D. The study showed that the 1D steady state

model performed almost as good as the others. Ji et al. [7] presented a dynamic model of the PV evaporator in a PV/T solar-assisted heat pump. The simulation results indicated that there was very small temperature difference distributed at the layers of PV module, aluminium sheet and refrigerant (neglecting the last small length of overheating) respectively. Therefore, for this work, the 1D steady state model is used for the simulation based on the following assumptions:

- The PV/T heat pump system is in quasi-steady state.
- The heat loss of the PV/T heat pump system is neglected.
- The pressure drop of the PV/T heat pump system is neglected.
- A mean temperature is assumed across each layer of the PV/T panel.

Based on the energy balance analysis of each component of the two PV/T panels and other components of the heat pump system, mathematic models are established for the numerical simulations on energy performance study.

The heat balance at the glass cover is given by

$$0 = \beta_g G + q_{r,p-g} + q_{v,p-g} - q_{v,g-a} - q_{r,g-sky} \tag{1}$$

where β_g is the absorbance of the glass cover "g"; $q_{r,p-g}$ is the heat radiation from the PV module "p" to "g"; $q_{v,p-g}$ is the heat convection from "p" to "g"; $q_{v,g-a}$ is the heat convection from "g" to the air; $q_{r,g-sky}$ is the heat radiation from "g" to the sky.

The energy balance at the PV module is given by

$$0 = (\beta\tau)_c G f_c + (\beta\tau)_p G(1 - f_c) - E - q_{d,p-al} - q_{r,p-g} - q_{v,p-g} \tag{2}$$

where $(\beta\tau)_c$ and $(\beta\tau)_p$ are the effective absorbance of the solar cells "c" and PV base plate, respectively; $q_{d,p-al}$ is the heat conduction from "p" to "al"; E is the electricity generation.

The heat balance at the aluminium sheet is given by

$$0 = q_{d,p-al} - q_{d,al-co} * \frac{A_{al-co}}{A_{al}} - q_{al-a} \tag{3}$$

where $q_{d,p-al}$ is the heat conduction from "p" to "al"; $q_{d,al-co}$ is the heat conduction from "al" to "co"; q_{al-a} is the heat transfer from "al" to the air; A_{al-co} is the contacting area between "al" and "co".

The heat balance at the copper tube is given by

$$0 = q_{d,al-co} A_{al-co} - q_{v,co-r} A_{i,co} \tag{4}$$

where $A_{i,co}$ is the internal surface area of "co"; $q_{v,co-r}$ is the heat convection from "co" to the refrigerant "r".

$$q_{v,co-r} = \frac{(T_{co} - T_r)}{\frac{1}{\alpha_r} + \frac{\delta_{co}}{2\lambda_{co}}} \tag{5}$$

where T_r is the refrigerant temperature; α_r is the convective heat transfer coefficient between "co" and "r", given by

For single-phase flow: $\alpha_r = 0.023 \frac{\mathrm{Re}^{0.8}\,\mathrm{Pr}^{a}\,\lambda_r}{d_i}$ (a=0.3 for liquid, a=0.4 for vapour) [8]

For two-phase flow: $\alpha_r = \alpha_l\left((1-x)^{0.8} + \frac{3.8x^{0.76}(1-x)^{0.04}}{\mathrm{Pr}^{0.38}}\right)$

where x is the average dryness fraction of the refrigerant. $\mathrm{Pr} = \frac{\mu_r Cp_r}{\lambda_r}$, $\mathrm{Re} = \frac{\rho_r u_r d_{i,co}}{\mu_r}$.

The heat balance at the refrigerant is given by

$$0 = q_{co-r} A_{i,co} - m_r \Delta h_r \tag{6}$$

where m_r is the mass flow rate of the refrigerant for each PV/T collector; Δh_r is the refrigerant enthalpy difference between collector inlet and outlet.

Neglecting the pressure drop in the discharge line, the relationship been the temperature and pressure at the discharge and suction sides of the compressor can be expressed by

$$T_{dis} = T_{suc}\left(\frac{p_{dis}}{p_{suc}}\right)^{\frac{\kappa-1}{\kappa}} \tag{7}$$

where T_{dis} and T_{suc} are the discharge and suction temperatures, respectively; P_{dis} and P_{suc} are the discharge and suction pressures, respectively.

The throttling process is regarded as the isenthalpic one. The mass flow rate is given by

$$m_r = k_{ex}\sqrt{\rho_r(p_{cd} - p_{ev})} \tag{8}$$

where k_{ex} is the characteristic constant of the valve; p_{cd} and p_{ev} are the condensing and evaporating pressure respectively; ρ_r is the density of refrigerant liquid.

The condensing temperature is kept at 45 ℃. The heat balance equations at the refrigerant side of the condenser are similar to that when it flows through the PV evaporator. At the water side of the condenser, the heat balance can be expressed by [8]

$$0 = m_w Cp_w\left(T_{w,out} - T_{w,in}\right) - \alpha_{w-hx} A_{w-hx}\left(T_{w,out} - T_{w,in}\right) \Big/ \ln\left(\frac{T_{hx} - T_{w,in}}{T_{hx} - T_{w,out}}\right) \tag{9}$$

where m_w is the water flow rate; Cp_w is the specific heat of water; $T_{w,out}$ and $T_{w,in}$ are the water temperature at the outlet and inlet respectively; α_{w-hx} is the convective heat transfer coefficient between water and the heat exchanger plate; A_{w-hx} is the contact area between water and the heat exchanger plate; T_{hx} is the temperature of the heat exchanger plate.

4. Results and analysis

Based on the above models, EES software is used to solve the mathematic models/equations. Numerical calculation is carried out under different solar radiation and constant air temperature of 15 ℃.

Fig. 3 shows the variation of thermal efficiency and condenser heat capacity under different radiations. It can be seen from Fig. 3 that both thermal efficiency and condenser heat capacity increased in linear with the increasing radiation. The condenser heat capacity increased more sharply than the thermal efficiency. When the radiation was 200 W/m2, the thermal efficiency and condenser heat capacity were 0.332 and 33.6 W, respectively. As the radiation increased to 1000 W/m2, the thermal efficiency and condenser heat capacity rose to 0.543 and 233 W, respectively. With every 100 W/m2 increase of radiation, the thermal efficiency increased by 0.03 and the condenser heat capacity increased by 24.9 W.

The average thermal efficiency and condenser heat capacity were 0.447 and 128.7 W, respectively.

Fig. 4 shows the variation of electrical efficiency and PV power output under different radiations. It can be seen from Fig. 4 that electrical efficiency dropped in linear with the increasing radiation and PV power output increased in linear with the increasing radiation. When the radiation was 200 W/m2, the electrical efficiency was 0.109 and the PV power output was 7.0 W. As the radiation increased to 1000 W/m^2, the electrical efficiency dropped to 0.071 and the PV power output increased to 22.8 W. With every 100 W/m^2 increase of radiation, the electrical efficiency dropped by 0.005 and the PV power output increased by 1.96 W. The average electrical efficiency and PV power output were 0.088 and 15.7 W, respectively.

Fig. 5 shows the variation of COP under different radiations. It can be seen from Fig. 4 that COP increased in linear with the increasing. When the radiation was 200 W/m^2, the COP was 3.6. As the radiation increased to 1000 W/m^2, the COP increased to 6.6. With every 100 W/m^2 increase of radiation, the COP increased by 0.38. The average COP was 5.1.

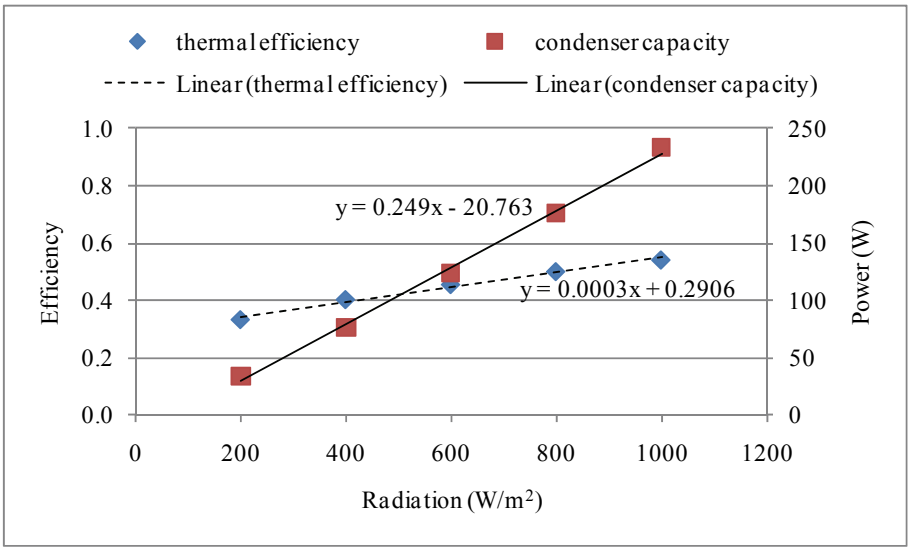

Fig. 3. Variation of thermal efficiency and condenser capacity with radiation.

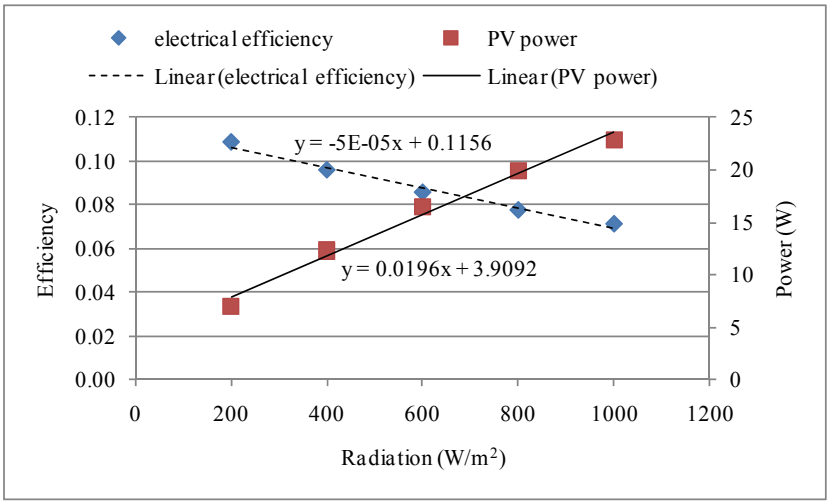

Fig. 4. Variation of electrical efficiency and PV power with radiation.

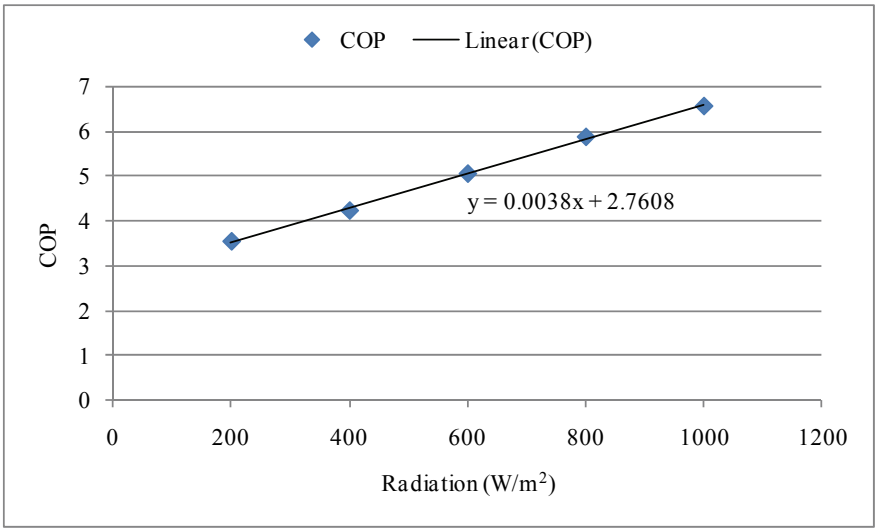

Fig. 5. Variation of COP with radiation.

5.Conclusions

A hybrid flat plate PV heat pump system was introduced in this paper. Numerical steady models have been established for each component of the heat pump system and part of the PV panel for the study on their energy performance. It can be concluded that:

- Both thermal efficiency and condenser heat capacity increased in linear with the increasing radiation. Thermal efficiency rose from 0.332 to 0.543 and condenser heat capacity rose from 33.6 W to 233 W, responding to the increasing radiation from 200 W/m2 to 1000 W/m2.

- Electrical efficiency dropped in linear with the increasing radiation and PV power output increased in linear with the increasing radiation. Electrical efficiency dropped from 0.109 to 0.071 and PV power output increased from 7.0 W to 22.8 W, responding to the increasing radiation from 200 W/m2 to 1000 W/m2.
- COP of the hybrid system increased from 3.6 to 6.6, responding to the increasing radiation from 200 W/m2 to 1000 W/m2.

Acknowledgements

The work of this paper was fully supported by Marie Curie Incoming International Fellowship (No. PIIF-GA-2009-234843).

References

[1] PVT forum. *PVT Roadmap – a European guide for the development and market introduction of PV-thermal technology*. 2006;<avaialbe at http://www.pvtforum.org/index.html>.

[2] Niccolo A, Giancarlo C, Francesco V. Design, development and performance monitoring of a photovoltaic-thermal (PVT) air collector. *Renewable Energy* 2008;**33**: 914–927.

[3] Tonui JK, Tripanagnostopoulos Y. Improved PV/T solar collectors with heat extraction by forced or natural air circulation. *Renewable Energy* 2007;**32**: 623–637.

[4] Dubey S, Tiwari GN. Thermal modeling of a combined system of photovoltaic thermal (PV/T) solar water heater. *Solar Energy* 2008;**82**: 602–612.

[5] Chow T, He W, Ji J, Chan ALS. Performance evaluation of photovoltaic–thermosyphon system for subtropical climate application. *Solar Energy* 2002;**81**:123–130.

[6] Zondag HA, de Vries DW, van Helden WGJ, et al. The yield of different combined PV-thermal collector designs. *Solar Energy* 2003;**74**:253–269.

[7] Ji J, He H, Chow T, Pei G, He W, Liu K. Distributed dynamic modelling and experimental study of PV evaporator in a PV/T solar-assisted heat pump. *International Journal of Heat and Mass Transfer* 2009;**52**:1365–1373.

[8] Duffie JA, Beckman WA. *Solar engineering of thermal processes*. Third edition, New York: Wiley; 2006.